Journal of Membrane Science 548 (2018) 421–428

Contents lists available at ScienceDirect

Journal of Membrane Science

journal homepage: www.elsevier.com/locate/memsci

Effect of temperature gradients in (reverse) electrodialysis in the Ohmic regime

Anne M. Benneker[a], Timon Rijnaarts[b,c], Rob G.H. Lammertink[a,b], Jeffery A. Wood[a,*]

[a] Soft matter, Fluidics and Interfaces, Faculty of Science and Technology, University of Twente, Enschede, The Netherlands
[b] Membrane Science and Technology Group, Faculty of Science and Technology, University of Twente, Enschede, The Netherlands
[c] Wetsus, Centre of Excellence for Sustainable Water Technology, Oostergoweg 9, 8911 MA Leeuwarden, The Netherlands

ARTICLE INFO

Keywords:
Waste heat utilization
(Reverse) Electrodialysis
Temperature gradient
Industrial desalination

ABSTRACT

Electrodialysis (ED) and reverse electrodialysis (RED) are processes for the production of desalinated water (ED) and power (RED). Temperature of the feed streams can strongly influence the performance of both processes. In this research, commercial membranes are used for the investigation of temperature and temperature gradients on ED and RED processes. We find that the energy required for ED processes can be reduced by 9% if the temperature of one of the feed streams is increased by 20 °C, while maintaining the charge-selectivity of the membranes. The direction of the temperature gradient did not have a significant influence on the efficiency and selectivity of ED in the Ohmic regime. In RED, we find an increase in obtained gross power density over 25% for the process when one feed stream is heated to 40 °C instead of 20 °C. This work experimentally demonstrates that utilization of low-grade waste heat from industrial processes can yield significant reduction of energy costs in ED processes, or result in higher power densities for RED systems where the increase in temperature of a single feed stream already yields significant efficiency improvements.

1. Introduction

Electrodialysis is a technique applied on industrial scale for the deionization of aqueous feed streams. In electrodialysis (ED), a membrane stack containing alternating anion (AEM) and cation exchange membranes (CEM) is used for the selective transport of ions by applying a potential gradient over the system [1], as is schematically shown in Fig. 1a. Anions will be transported through the AEM and blocked by the CEM, while for the cations the opposite is true, resulting in an ion enriched (concentrate) and an ion depleted (diluate) stream at the outlet of the stack [2]. ED is applied on an industrial scale in the treatment of aqueous solutions for various applications such as desalination for drinking water, nitrate removal, salt removal from protein and sugar solutions and the deionization of whey [1]. In commercial systems, ED is operated in the so-called Ohmic regime, to prevent concentration polarization and minimize pressure drops in the solution adjacent to the membrane [3].

In reverse electrodialysis (RED), as the name suggests, the opposite is occurring as the energy of mixing two streams with different inlet salt concentrations is harvested in a membrane stack, as schematically depicted in Fig. 1b. RED processes can be of use at natural points where two streams containing different salt concentrations are contacting, such as for instance river estuaries (low salt concentration) in the sea (high salt concentration) [4–7], or in hypersaline brines [4]. RED processes are currently being tested at lab and pilot plant scales [8].

Both ED and RED have been studied extensively in the past decades [1,9–11], regarding membrane selectivity and optimizing flow patterns adjacent to the membranes as two prominent goals to improve the efficiency of both processes. Typically, most commercial membranes exhibit a selectivity above 90% [10]. Ion transport from the liquid phase to the membrane is of large influence on the efficiency of ED and RED, and partially determines the required or obtained potential. Transport can be enhanced by continuously mixing the solution in order to reduce the development of an ion depleted boundary layer or by enhancing the transport of ions in the solution. Optimization of the flow patterns can be achieved using profiled membranes or spacers [12–14]. In both ED and RED, there is transport of water as a result of the osmotic gradient. This water transport results in a drastic reduction in efficiency of the process [15], most significantly in ED-processes. For cation exchange membranes, the direction of the water transport in systems where only a temperature gradient is applied (no applied potential gradient) depends on the coupling between the electrolyte and the water [16–18]. If only an osmotic gradient is present, water transport will be from the solution with a low salt concentration

* Corresponding author.
E-mail address: j.a.wood@utwente.nl (J.A. Wood).

https://doi.org/10.1016/j.memsci.2017.11.029
Received 22 September 2017; Received in revised form 3 November 2017; Accepted 11 November 2017
Available online 13 November 2017

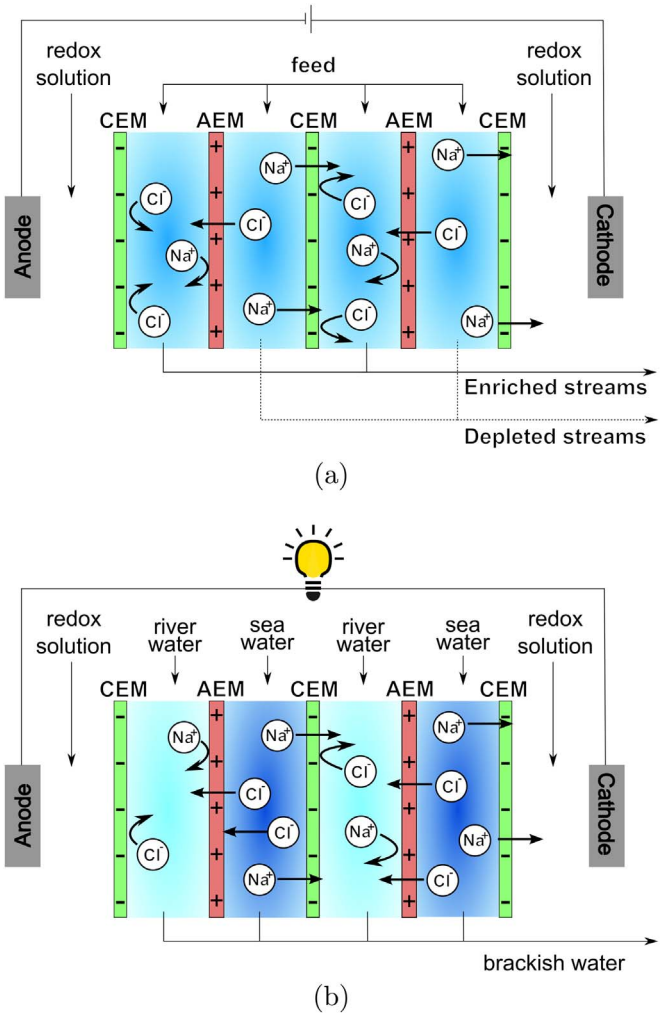

Fig. 1. (a) Schematic representation of an electrodialysis (ED) stack, in which equi-concentrated feed streams are separated in a concentrated and diluted stream under the influence of an externally applied electric field. (b) Schematic representation of a reverse electrodialysis (RED) stack, in which two streams with different ionic strengths are fed through compartments between alternating cation and anion exchange membranes and electricity is produced as a result of concentration-gradient induced ion transport. In both systems, the electrodes are flushed with a redox solution, providing electrons for charge transport and to avoid gas formation.

towards the higher salt concentrations, therefore in the opposite direction of ion transport [16]. In addition to osmosis, there is water transport as a result of electroosmotic flows, in which the water is transported alongside the ions that are moving as a result of the electric field. In ED, the direction of electroosmotic transport of water is the same as the osmotic water transport, while in RED they are in opposite directions [19]. The efficiency losses as a result of water transport are reported to increase with increasing concentration differences and increasing temperature in the system [15,20]. Elevated temperatures can yield additional limitations in the process, such as the degradation of the membrane material and the precipitation of low solubility compounds on the membranes [21]. On the contrary, elevated temperatures might yield a lower energy requirement for the ED process [22] and can enhance the obtainable power from RED processes [10].

When a temperature gradient is applied over a membrane separating two solutions of equal salt concentration, a thermal membrane potential is measured, indicating a thermoelectric effect over the membrane [23–26], which can be harvested as electric work [24,27,28], similar to the RED principle. Additionally, a thermoosmotic water flux might be established [29,18,30], of which the direction is dependent on the membrane at hand [16]. It is stressed that this temperature gradient does not necessarily result in the development of a concentration gradient over the membrane [25]. If, in addition to the temperature gradient a potential or concentration gradient is applied over the membrane, the selective transport of ions might be enhanced by the coupling of effects resulting from temperature gradients with the other transport phenomena in the system. When the temperature gradient in ED is applied in the same direction as the electric field, the relative flux of counter-ions can be enhanced when compared to the co-ion flux, increasing the efficiency of the separation of ions from the solution [31]. The total ionic current can be increased if temperature gradients or elevated temperatures are applied over the membrane, as a result of the increased diffusivity of ions in the solution [31,32]. Experimental [33,34] and theoretical [35] investigations have shown that elevated temperatures are beneficial for the obtainable power density in RED systems with highly saline feed solutions, albeit at isothermal conditions. The effect of temperature gradients in realistic ED and RED set-ups also containing a salt or potential gradient have, to the best of our knowledge, not been investigated experimentally. These situations are interesting for applications where there is a natural temperature gradient between two inlet feed streams, e.g. where a river meets a sea, or for industrial plants that deal with low-grade waste heat. Moreover, applying a temperature gradient vs. isothermal operation may reduce the negative side-effects of high temperature operations, such as scaling and increased water transport [21].

In this paper, we experimentally study the effect of imposed temperature gradients in ED and RED systems. We measure the required power for desalination in ED in the industrially relevant Ohmic regime, as well as the obtained power density from the RED system under various temperature settings. The temperature settings are chosen as such that they are obtainable by utilizing waste heat for heating the feed streams. Additionally, we measure ion concentrations to investigate the effect of temperature gradients on the selectivity of membranes and the efficiency of the ED system. Our experiments show that we can enhance the energy efficiency of ED systems by working with temperature gradients and at elevated temperatures, and improve the power density of RED systems in the same manner. The selectivity for ion transport remained constant, meaning there was no loss of membrane selectivity and functionality at elevated temperatures. These results show the potential use of waste heat to improve either desalination or power generation in ED and RED processes.

2. Experimental details

Experiments were performed using a cross-flow RED stack, with an active area of 10 × 10 cm^2, provided by REDstack BV (The Netherlands). The two feed inlet streams are perpendicular to each other, resulting in a relatively high heat transfer between the two streams which are in cross-flow configuration. Four cell-pairs consisting of commercially available cation and anion exchange membranes with an intermembrane distance (channel height) of 260 μm were assembled in the stack. The membranes used are Neosepta® CMX and Neosepta® AMX (obtained from Eurodia, France), which are punched to size using an in-house build mold. The 260 μm thick spacers with a free volume of 0.726 and a free surface fraction of 0.476 were provided by Deukum GmbH (Germany). End-plates were tightened using screws and the side-plates of the RED stack were sealed. Electrical measurements are done using a Metrohm Autolab PGSTAT302N equiped with a FRA module (Metrohm Autolab, The Netherlands), which is controlled by NOVA 2.0 software. Current or potential was applied through Pt coated Ti electrodes (provided by Magneto Special Anodes BV, The Netherlands), located in the stack end plates.

Both ED and RED experiments are done at four different temperature configurations; (1) isothermal at 20 °C, (2) feed 1 at 20 °C, feed 2 at 40 °C, (3) feed 1 at 40 °C, feed 2 at 20 °C and (4) isothermal at 40 °C, as is summarized in Table 1. Feed solutions were kept at the desired temperatures using two Julabo F12-ED Refrigerated - Heating

Table 1
Tested temperature configurations in ED and RED experiments.

Case	T_D (river) [°C]	T_C (sea) [°C]
Cold isotherm	20	20
Hot concentrate	20	40
Hot diluate	40	20
Hot isotherm	40	40

Circulators. The system was allowed to settle to thermal equilibrium and outlet temperatures were measured using AMA-digit ad 15th thermometers (Amarell, Germany) before and after the electrical measurements.

All measurements are done at a constant flow rate of 50 mL/min, which corresponds to a flow speed (linear flow velocity) of 0.81 cm/s in the compartments. Flow was pumped using peristaltic pumps (Cole-Parmer) and flow pulsations were suppressed using in-house built pulsation dampeners. The flow rate was controlled using an in-house built flow meter (TCO, University of Twente, The Netherlands), containing a McMillan Co. 101 flo-sen flow sensor. The membrane packing was ensured by applying an 0.1 bar overpressure on the electrolyte stream (flow rate was adjusted accordingly), using a simple needle valve.

2.1. Electrodialysis

For experiments in the electrodialysis (ED) mode a feed solution of 1 g/L NaCl (0.017 M) is pumped through all compartments of the stack. The electrolyte used in ED mode contained 0.017 M NaCl and 0.1 M $K_4Fe(CN)_6$ and 0.1 M $K_3Fe(CN)_6$ as the redox pair. All chemicals were obtained from Sigma Aldrich (the Netherlands). Both depleted and enriched outlet streams are recycled into the feed container, which is continuously mixed using aquarium mixers (Wavereef®Auto Top Off System, Single Level Sensor WIC-01S, obtained from Aquaria Veldhuis BV, The Netherlands). The system was allowed to equilibrate in temperature before measurements were started.

Constant current measurements (chronopotentiometry) are done at a current of 0.15 A, corresponding to 15 A/m^2, which was confirmed to be in the Ohmic regime of this stack (by measuring IV responses) to avoid any influences of concentration polarization on the measurements as the goal of these experiments was the investigation of temperature gradients in the Ohmic regime. The required potential to sustain this current is measured for 600 s.

Samples are taken during the measurements to evaluate the salt concentrations in the outlet streams by means of ion chromatography (IC). Conductivity of inlet and outlet streams was monitored during the experiments using a WTW Cond 3310 conductivity meter equiped with a WTW Tetracon 325 sensor (WTW, Germany), to check if depletion and enrichment of the streams is as expected. Anion concentrations were quantified with IC (Metrosep A Supp 16 - 150/4.0 column on a Metrohm 850 Professional IC). Cation concentrations were measured with IC as well (Metrosep C6 - 150/4.0 column on a Metrohm 850 Professional IC).

2.2. Reverse electrodialysis

Reverse electrodialysis experiments were done with model solutions of 30 g/L (0.513 M,“sea water”) and 1 g/L (0.017 M, “river water”) through the different compartments. The electrolyte used in RED mode contained 0.25 M NaCl and 0.1 M $K_4Fe(CN)_6$ and 0.1 M $K_3Fe(CN)_6$ as the redox pair. No recycling of the outlet streams is done in these experiments, as the salt gradient is reduced during the measurement. The pressure drop in both sea and river water streams was monitored between the inflow and the outflow of the solutions, using a differential pressure meter (Endress + Hauser Deltabar S, Germany).

Different parameters were measured during a single RED measurement. Open circuit voltage (OCV) was measured prior and after the stack resistance measurements (both AC and DC mode). The total stack resistance is a result of the Ohmic resistance (resulting from the resistance of the feed streams and the membranes) and the non-Ohmic resistance (caused by concentration changes due to ionic transport). To be able to uncouple the Ohmic resistance from the total stack resistance, measurements in AC mode are required. In AC measurements there is no net ionic current due to the alternating direction, which does not cause these non-Ohmic effects [34]. For determination of the Ohmic stack resistance, alternating currents with a frequency between 1 and 10 kHz are applied, while measuring the impedance. Total stack resistance is measured in DC mode (direct current, 17 steps of 40 s each, from 0 to 40 A/m^2 and back), and the non-Ohmic resistance is calculated as the difference between the total and Ohmic resistance of the stack. A blank measurement is done to determine the resistance of the electrolyte and the outer CMX membrane, in which no salt solutions are fed.

3. Results and discussion

3.1. Temperature profile development in the system

In our measurements, we controlled the inlet temperature of both feed streams and measured the outlet temperatures. For the non-isothermal cases, we found that the cold feed stream (independent of its salt concentration) had a higher outlet temperature (~32 °C) than the outlet of the hot feed stream (~28 °C). This indicates a high amount of heat exchange between the two streams, as was expected. Note that we measure the average outlet temperatures of both streams, and are not able to record local temperatures inside the stack. For isothermal systems, both hot and cold, the outlet temperatures of both streams were equal. For the low temperature isothermal cases, the streams showed a slight increase in temperature, to ~ 22 °C, while for the isothermal high temperature case, the outlet streams were cooled down to ~ 32 °C due to the temperature of the surroundings of ~ 25 °C. Heat is conducted well through our, mostly steal, membrane stack. Thermal insulation is present around the reservoir and the feed tubes towards the stack, but not the total stack. Thermal insulation of the total stack would prevent leakage of heat, but also inhibit our visual observations of the bubble formation in the stack as a result of the elevated temperatures. By measuring both the in- and outlet temperatures of the stack we obtain an estimate of the heat losses to the surroundings which are taking into account in our model.

In order to estimate the local temperature profile within the stack, the following partial differential equations (Eq. (1)) were solved in MATLAB using polynomial collocation with a Chebyshev polynomial basis [36]. This model is a simple extension of the existing cross flow heat exchange temperature profile model to include heat losses to the environment from both the cold and hot streams [37]. In this approach, the heat losses/gains from the environment are approximated as being proportional to the temperature difference between each respective stream (river/sea) and the environment (treated as a constant wall temperature). Qualitatively similar results are obtained from the 2D analytical solution without heat loss, particularly with respect to the average temperature difference between the hot and cold streams at any given point in the stack [37].

$$\frac{\partial T_C}{\partial x} = \frac{kA}{mC_pXY}(T_H - T_C) + \frac{hA}{mC_pXY}(T_{wall} - T_C)$$
$$\frac{\partial T_H}{\partial y} = \frac{-kA}{mC_pXY}(T_H - T_C) + \frac{hA}{mC_pXY}(T_{wall} - T_H) \quad (1)$$

In Eq. (1) k is overall heat transfer coefficient between hot and cold streams, h is the heat transfer coefficient to the environment, A the heat exchange area, m is the mass of fluid in the respective stream (in this

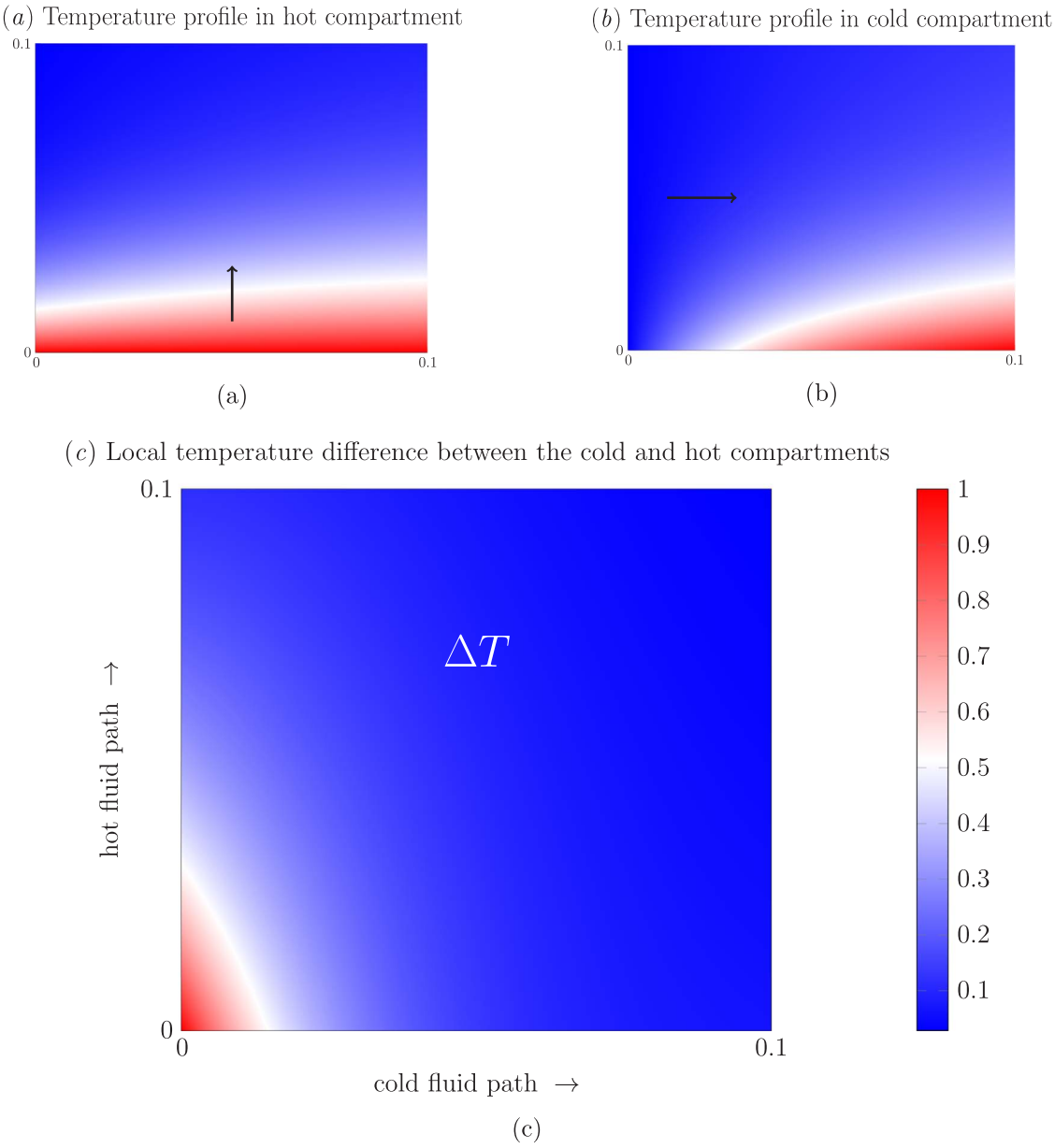

Fig. 2. Temperature profiles inside the stack, resulting from numerical calculations of local temperatures. Temperature in the hot stream, θ_H (a) (flow from bottom to top, as indicated by arrow) and temperature in the cold stream, θ_C (b) (flow from left to right, indicated by arrow) as a function of location in the stack. (c) Local temperature difference ($\theta_H - \theta_C$) between hot and cold streams, indicating a positive temperature gradient in all locations of the stack.

case equal for hot and cold and equal to the flowrate multiplied by residence time), C_p the heat capacity and X and Y represent the length of the x and y path respectively. hA is estimated based on the measured values for the in- and outlet temperatures, together with our relevant system parameters, and is found to be hA = 3 J. m/K. kA is estimated based on the flow rate in our system and assumed to be 2.35 J. m/K. Using these values, a local temperature profile within the stack can be estimated. The average outlet temperatures are compared with the experimentally measured outlet temperatures and are in good agreement.

Results from this model are shown in Fig. 2, which shows the dimensionless temperatures ($\theta = (T - T_{C,in})/(T_{H,in} - T_{C,in})$, with T as the local temperature, $T_{H,in}$ and $T_{C,in}$ as the respective hot and cold inlet temperatures) in the hot and cold streams along with the difference. From our model, we can predict a temperature gradient in the same direction at all locations in the stack (see Fig. 2c). At the outlets, the temperature difference is dramatically reduced when compared to the difference in inlet temperatures. The temperature profiles for both hot (flow in vertical direction, from bottom to top) and cold (flow in horizontal direction, from left to right) streams are shown as well, from which one can see that the cold stream is heated mostly at the side at the inlet of the hot stream (left in Fig. 2b). The hot stream is, as is expected, cooled down the most at the inlet side of the cold stream (bottom of Fig. 2a).

3.2. Electrodialysis

Six measurements were done at every temperature configuration shown in Table 1. During the first three measurements no samples were taken to not disturb the flow patterns in the system, while samples were taken during the additional measurements. Results of the constant current measurements (I = 0.15A which corresponds to a current density of 15 A/m^2), for which the potential was recorded, are shown in Fig. 3. As can be observed, there is a distinct difference between the different temperature configurations, as is expected. The highest

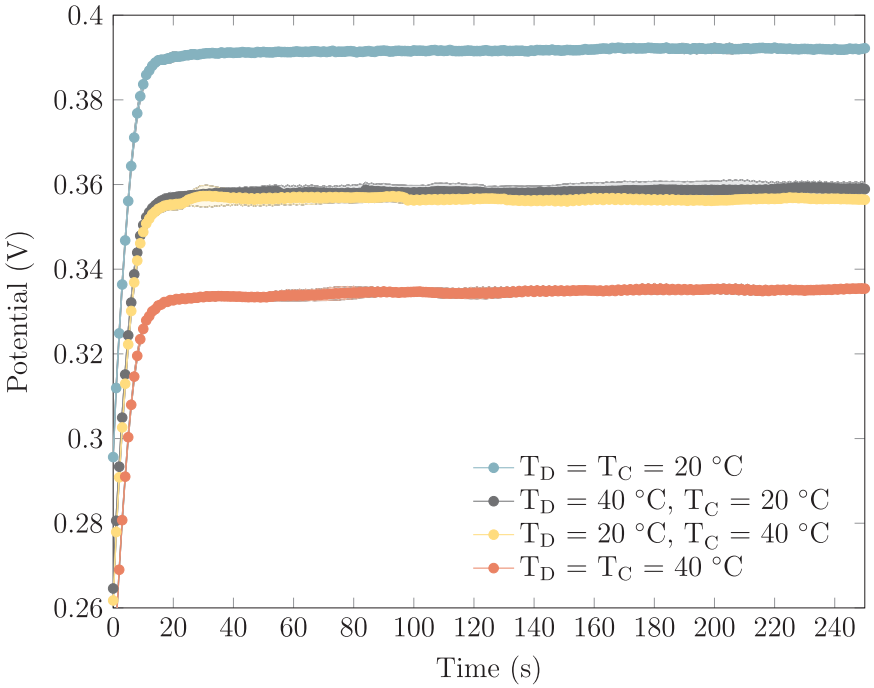

Fig. 3. Potential required to obtain a constant current of 15 A/m^2 in ED mode in the different temperature configurations. Lines are for indication purposes only. Error bars (very small) are the standard deviation between the measurements.

potential is required for measurements with an isothermal low temperature, while the lowest potential is required for measurements with an isothermal high temperature. The cases in which there is a temperature gradient applied require a moderate potential for the same current, but no significant difference between the two directions of the temperature gradient was measured. The variance between the different measurement runs (six per temperature configuration), were very small (a relative error of ~ 2% at maximum).

The settling time for the potential to become stable is ~ 20 s, after which the potential becomes very stable. This indicates that we are in the Ohmic regime and the current is still linearly dependent on the potential that is applied, which was also confirmed by an IV-sweep of the total stack, where the transition from the Ohmic regime towards the limiting regime is observed around 0.24 A (24 A/m^2).

Most of the drop in required potential for the transport of current can be explained by the altered diffusivity of ions at higher temperatures. If the temperature of the feed is higher, the diffusivity (and therefore the conductivity) of the solution is increased, and thus the resistance of the total stack is reduced. The conductivity of the solution is increased by approximately 27% [38] at 40 °C, which is also approximately the drop in required potential. Surprisingly, our potential measurements did not show a significant difference between the measurements in which a temperature gradient was applied, which we mainly attribute to the efficient heat transfer between the different flow compartments leading to a smaller gradient vs. inlet conditions, as was discussed in the previous section.

To establish if the imposed temperature (gradient) has an influence on the selectivity of the membranes or the ratio between cation and anion fluxes, samples were taken of both streams during the measurements around t = 300 s. Both cation and anion concentrations in these streams were measured. For cations, there were significant concentrations of Na^+ and K^+ in the outlet streams. The presence of K^+ is a result of cation exchange with the electrolyte, in which K^+ is the main cation. The inlet concentration that was measured is slightly higher than the feed concentration of salt at the start of the experiments (0.020 M versus 0.017 M), which is also contributed to the flux of ions from the electrolyte towards the salt solution. Total inlet cation concentration (measured at the end of all experiments) is compared to the total outlet cation concentration, consisting of both measured cations. From the anion analysis only Cl^- ions were found to be present in the solution. The total average concentration of the outlet streams was increased, also as a result of a concentration gradient between the electrolyte solution and the feed solutions, which results in leakage of the ions towards the salt solutions.

No significant difference in the outlet ion concentrations for the different temperature configurations was found. Measured values are shown in the Supplementary Information. This indicates that there is no significant loss of selectivity of the membranes in the case of elevated temperatures and temperature gradients, but also no enhancement. We attribute this to the fact that we operate in the commercially relevant Ohmic regime, where we only expect minimal changes for the different configurations depending on how close to the limiting plateau the system is operated. The absence of concentration polarization inhibits any differences in ion transport between the different temperature configurations. Surprisingly, the temperature (gradients) do not significantly influence the water transport through the membranes either, which is unlike expectations based on previous results [16]. This is beneficial for the efficiency of the process and enables the application of temperature gradients in commercial systems. Cation concentrations are consistently higher than anion concentrations (in both depleted and enriched streams) which is attributed to the preferential leaking of cations from the electrolyte to the feed solution through the outer CMX membranes and the existence of additional anions in the system which are not measured in IC measurements, such as HCO_3^-. With the in- and outlet concentrations (C_{in} and C_{out}), the so-called desalination degree $(1 - C_{out}/C_{in}) \times 100\%$ [39] can be calculated, yielding a desalination degree of ~ 35% for cations for all cases. The desalination degree is similar for all configurations (as was expected due the equal current that was applied for all configurations), as the outlet concentrations are not significantly different for the different configurations.

Another indicator of performance is the current efficiency of desalination [40];

$$CE = \frac{zFQ_f(C_{in} - C_{out})}{NI} \times 100\% \quad (2)$$

where Q_f is the diluate flow rate (m^3/s), F is Faradays constant, z the ion valency, N is the number of cell pairs and I is the current (A). This current efficiency is an indicator of the amount of current that is being

used for effective ion transport. A current efficiency lower than 100% indicates the undesired transport of additional charge carriers (such as H^+ or OH^-) or the existence of shortcut currents in the system. For our measurements, the current efficiency is ~ 100%, for both cations and anions, indicating that all current is used for selective transport of Na^+ and Cl^- ions. This high value is a result of measuring in the Ohmic regime, in which there are no significant limitations in ion transport and water splitting is not significant. Enhancing the diffusivity in the diluted channel is not of larger influence than enhancing the diffusivity in the enriched channel, which is counter to our initial expectations [16,31]. At higher currents, in the so-called limiting and overlimiting current regime [1,41], we expect the current efficiency to change for the different temperature configurations as a result of the increased diffusivity of the ions at higher temperatures. In the limiting current regime, concentration polarization over the membrane results in an enhanced resistance for ion transport, limited by the (diffusive) transport of ions towards the membrane. If temperature is increased, the transport of ions towards the interface is enhanced, resulting in a higher current efficiency, which would be interesting for future experiments.

The total power ($P = UI$) required for desalination can be calculated for the different temperature configurations. As the current was kept constant, the only variable in this equation is the required potential U (Fig. 3). This potential was highest for the low temperature isothermal case and lowest for the high temperature isothermal case. Based on the average potential required in the steady state of our 50 mL/min measurements, the power required for the low temperature isothermal case is highest ($P = 58.7$ mW) and is reduced by ~ 15% for the high temperature isothermal case ($P = 50.1$ mW). The cases in which there is a temperature gradient require intermediate power (~$P = 53.5$ mW for both cases). Heating up one of the feed streams reduces the required power by ~ 9%, independent on the composition of the hot stream. As the depletion and enrichment of the different ions did not differ between the different cases, it can be concluded that the pre-heating of (one of the) feed streams for ED processes can reduce the power input in these processes. The heat that it would require to increase the feed temperature of both streams accounts to 140 W, and is significantly higher than the reduction in electric power that is obtained. However, process plants usually need to cool down process streams before they can be discharged into rivers, and the ED process efficiency can potentially be enhanced by utilizing this waste heat for increasing the temperature of the feed streams [42,43]. Of course, the effects of elevated temperatures on membrane fouling and lifetime should be investigated in more detail as well before any conclusions for implementation can be drawn.

3.3. Reverse electrodialysis

From the measurements in RED mode, the gross power density (GPD in W/m^2) can be calculated using the measured current (I) and potential (U), which is corrected for the resistance of the electrolyte by subtraction of U_{blank} and the total membrane area inside the four cell pairs (A).

$$GPD = \frac{I(U - U_{blank})}{A} \tag{3}$$

The calculated GPD as function of current density is plotted in Fig. 4 for the different temperature configurations. As expected, the maximum GPD is increased for the cases in which at least one of the feed streams has an elevated inlet temperature. In the most extreme case, the total maximum GPD is increased with almost 38% (from 0.68 W/m^2 at $T = 20$ °C to 0.94 W/m^2 at $T = 40$ °C), while if only one stream is heated the total maximum GPD is increased by over 25% to 0.85 W/m^2. The current density at which this maximum GPD is found is also shifting when temperatures are increased in the system, which is beneficial for the total energy that can be harvested from the RED stack.

Measured and fitted (from IV data) values for the open circuit voltage (OCV in V) are reported in Table 2. The OCV is the potential difference over the membrane stack as a result of the imposed ion concentration gradients, when there is no current and no losses due to concentration gradients in the system. For the low temperature isothermal case, the measured OCV is 0.60 V and it increases when a temperature gradient is applied, just as is expected. Consistently, the measured OCV is slightly higher than the fitted OCV, as this results from fitting with data points at the other applied currents. The measured OCV values can be compared to theoretical values that are expected for a stack of four cell pairs, based on the Nernst equation;

$$E_{cell} = \frac{RT}{zF}\alpha_{CEM}\ln\left(\frac{\gamma_c c_c}{\gamma_d c_d}\right) + \frac{RT}{zF}\alpha_{AEM}\ln\left(\frac{\gamma_c c_c}{\gamma_d c_d}\right) \tag{4}$$

using the activity coefficients of the ions in both concentrate and diluate streams (γ_c and γ_d, see Appendix A), the ion concentrations (c_c and c_d), the operating temperature (T) and the universal gas constant (R). The effect of temperature on the activity coefficients for 1:1 salts was treated as negligible in this temperature range, as per previous results [44]. For an actual cell, this potential has to be corrected for the non-perfect permselectivity of the membranes using the correction factors $\alpha_{CEM} = 0.907$ and $\alpha_{AEM} = 0.970$.

For simplicity, we have calculated the expected Nernst potential at both 20 and 40 °C, and have not incorporated the temperature gradient in the Nernst equation, as the thermoelectric potential generated by the temperature gradient is expected to be on the order of a few mV at most [24,25]. At $T = 20$ °C the expected cell potential is 0.146 V (compared to a measured cell potential of 0.150 V), while at $T = 40$ °C this potential is increased to 0.161 V (measured cell potential of 0.155 V). The differences in measured and predicted values can be explained by slight variations in the temperature during experiments, yielding an overestimation of the cell potential at high temperatures and an underestimation of the cell potential at low temperatures.

Another important parameter for RED is the electrical resistance of the stack, as this determines the efficiency of the system and the potential power generation with it. The total impedance of the stack can be split into an Ohmic and a non-Ohmic part. The Ohmic resistance of the stack consists of both AEM and CEM resistance, as well as the resistances in the feed streams, $R_{Ohmic} = R_{CEM} + R_{AEM} + R_{RW} + R_{SW}$ and can be measured using the AC mode of the potentiostat, while the total resistance is measured in DC mode. The non-Ohmic resistance can be calculated as the difference between the measured total and Ohmic resistance. All resistances are shown in Table 2, and it is clear that the total resistance of the stack goes down with increasing temperature. This mostly is a result from a lower Ohmic resistance, which results from the increased diffusivity of ions in both feed streams (reduction of R_{RW} and R_{SW}) and thus the enhanced ion transport in the solutions. For example, at the average temperature in the stack for inlet temperatures of $T_D = T_C = 40$°C, the river water resistance is decreased by approximately 27% [38] and a similar value is expected for the sea water [45]. The resistance of CMX and AMX membranes is also expected to decrease by approximately this amount based on previous literature [46] and this is also the observed percent reduction in the total Ohmic resistance vs. an inlet of 20 °C for both channels. The non-Ohmic resistance of the stack increases with an increase of temperature in the stack due to higher capacitive effects of the solution at higher temperatures. As a result of this, a larger concentration gradient is developed in the direction of the flow because of the larger charge transport in these cases, which results in a higher non-Ohmic resistance in the system [47].

The net power density that can be obtained with the RED stack can be calculated using the GPD and the losses that are present as a result of pressure drops over the effluent channels. The pressure drop was measured to be 25 mbar on average, and the applied flowrate was 50 mL/min (0.81 cm/s) for both compartments. We did not find a significant change in pressure drop for the different temperature

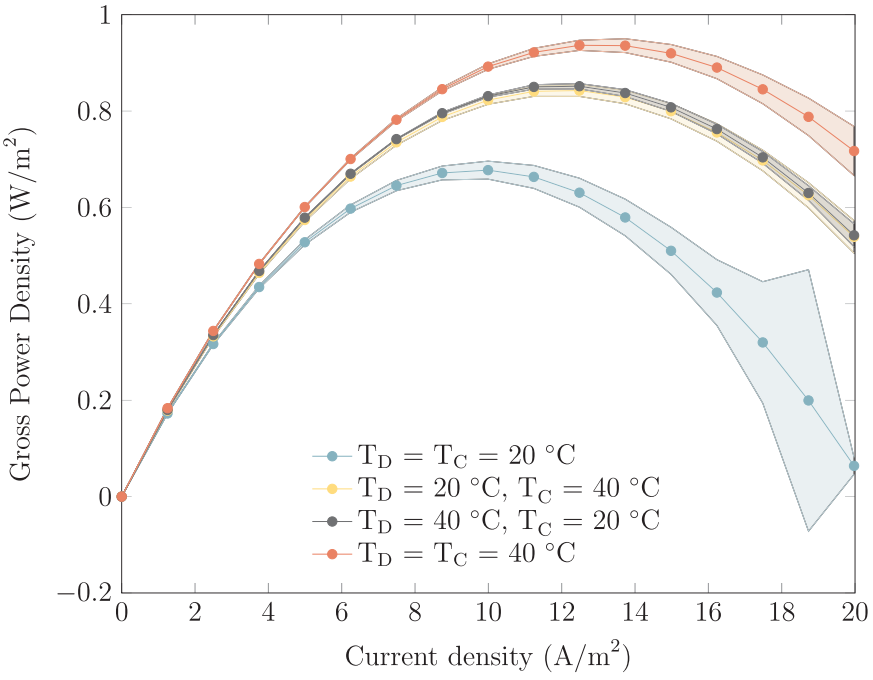

Fig. 4. Gross power density as function of the applied current density in the RED-stack for different temperature configurations. The maximum GPD increases with increasing temperature, while the current density at which this maximum occurs also shifts upwards. Lines are for indication purposes only. Errors are calculated using the propagation of errors theory.

Table 2
Open circuit voltages and stack resistances for different temperature configurations. Our stack consisted of four cell pairs. Errors in measured values are standard deviations, errors of calculated values are standard errors (given between brackets).

	$T_D = T_C = 20$ °C	$T_D = 20$ °C, $T_C = 40$ °C	$T_D = 40$ °C, $T_C = 20$ °C	$T_D = T_C = 40$ °C
OCV_{meas}[V]	0.60 (5.8×10^{-4})	0.61 (1.5×10^{-3})	0.62 (5.8×10^{-4})	0.62 (1.5×10^{-3})
OCV_{fit}[V]	0.57 (2.5×10^{-3})	0.59 (2.1×10^{-3})	0.59 (2.0×10^{-3})	0.60 (2.0×10^{-3})
$R_{total}[\Omega]$	1.59 (1.1×10^{-2})	1.38 (8.7×10^{-3})	1.39 (8.7×10^{-3})	1.33 (8.4×10^{-2})
$R_{Ohmic}[\Omega]$	1.56 (3.5×10^{-2})	1.30 (1.7×10^{-2})	1.29 (1.6×10^{-3})	1.19 (6.1×10^{-3})
$R_{Non-Ohmic}[\Omega]$	0.03 (7.0×10^{-4})	0.08 (1.2×10^{-3})	0.10 (6.4×10^{-4})	0.14 (8.9×10^{-3})

configurations. The net power density is highest for the case where there is a high temperature, indicating that by heating the inlet streams, the efficiency of the RED stack can be enhanced.

4. Conclusions

In this study, we have investigated the effect of imposed temperature gradients on ED and RED performance. We have experimentally demonstrated that the power input for electrodialysis processes for desalinating sea water can be reduced by ~ 15% if the temperature of the inlet streams are increased from 20 °C to 40 °C. Surprisingly, selectivity of the used commercial membranes and the degree of desalination are not significantly affected if the temperature is increased. An imposed temperature gradient over the membranes in the stack did also increase the desalination efficiency, since the power input was reduced by ~ 9%, although we measured no significant influence of the direction of the imposed temperature gradient in combination with the direction of the electric field in the Ohmic regime. The reduced power input can be attributed mainly to reduced stack resistance as a result of elevated diffusivity of the ions caused by an elevated temperature. This indicates that by using low-grade waste heat to heat even a single inlet stream in an ED process, the total required power to produce desalinated water can be decreased. Heating only one of the streams can also potentially reduce the negative effects of working at elevated temperatures, such as scaling and fouling [21].

In reverse electrodialysis, the gross power density was increased with ~ 38% as a result of an increased temperature from 20 °C to 40 °C. If a temperature gradient is imposed, the GPD increased by ~ 25%. The Ohmic resistance of the stack decreases for higher temperatures, which results in a higher obtainable current and thus a higher gross power density. The current density at which the maximum power density is obtained is shifted upwards with increasing temperature. No significant difference in power generation was determined based on the direction of the temperature gradient at the conditions studied, although this may not be the case when considering mixtures including multivalent ions or if membrane permselectivity is changing with temperature.

Acknowledgements

The authors thank Ehsan Reyhanitash (Sustainable Process Technology group, University of Twente) for his help with ion chromatography. This research was financially supported by the European Research Council, under the ERC starting grant 307342-TRAM awarded to R.G.H. Lammertink. The authors would also like to thank the participants of the research theme 'Blue Energy' at Wetsus, The Netherlands for their support.

Appendix A. Activity Coefficient Data for NaCl

Table 3

Table 3
Activity coefficients used for calculation of Nernst potential in RED [48].

Ion	Concentration [M]	γ_i
Na^+	0.5	0.614
Cl^-	0.5	0.651
Na^+	0.017	0.873
Cl^-	0.017	0.878

Appendix B. Supplementary data

Supplementary data associated with this article can be found in the online version at http://dx.doi.org/10.1016/j.memsci.2017.11.029.

References

[1] H. Strathmann, Electrodialysis, a mature technology with a multitude of new applications, Desalination 264 (3) (2010) 268–288.
[2] F.G. Helfferich, Ion Exchange, McGraw-Hill, 1962.
[3] W.A. McRae, Electroseparations, Electrodialysis, John Wiley and Sons, Inc., 2000.
[4] G.L. Wick, Power from salinity gradients, Energy 3 (1) (1978) 95–100.
[5] R.E. Lacey, Energy by reverse electrodialysis, Ocean Eng. 7 (1) (1980) 1–47.
[6] R. Pattle, Production of electric power by mixing fresh and salt water in the hydroelectric pile, Nature 174 (4431) (1954) 660.
[7] J.N. Weinstein, F.B. Leitz, Electric power from differences in salinity: the dialytic battery, Science 191 (4227) (1976) 557–559.
[8] J.W. Post, C.H. Goeting, J. Valk, S. Goinga, J. Veerman, H.V.M. Hamelers, P.J.F.M. Hack, Towards implementation of reverse electrodialysis for power generation from salinity gradients, Desalin. Water Treat. 16 (1–3) (2010) 182–193.
[9] J.W. Post, H.V.M. Hamelers, C.J.N. Buisman, Energy recovery from controlled mixing salt and fresh water with a reverse electrodialysis system, Environ. Sci. Technol. 42 (15) (2008) 5785–5790.
[10] P. Długołęcki, A. Gambier, K. Nijmeijer, M. Wessling, Practical potential of reverse electrodialysis as process for sustainable energy generation, Environ. Sci. Technol. 43 (17) (2009) 6888–6894.
[11] J.G. Hong, B. Zhang, S. Glabman, N. Uzal, X. Dou, H. Zhang, X. Wei, Y. Chen, Potential ion exchange membranes and system performance in reverse electrodialysis for power generation: a review, J. Memb. Sci. 486 (2015) 71–88.
[12] D.A. Vermaas, M. Saakes, K. Nijmeijer, Power generation using profiled membranes in reverse electrodialysis, J. Memb. Sci. 385–386 (1) (2011) 234–242.
[13] S. Pawlowski, V. Geraldes, J.G. Crespo, S. Velizarov, Computational fluid dynamics (CFD) assisted analysis of profiled membranes performance in reverse electrodialysis, J. Memb. Sci. 502 (2016) 179–190.
[14] D.A. Vermaas, M. Saakes, K. Nijmeijer, Enhanced mixing in the diffusive boundary layer for energy generation in reverse electrodialysis, J. Memb. Sci. 453 (2014) 312–319.
[15] W.J. van Egmond, M. Saakes, S. Porada, T. Meuwissen, C.J.N. Buisman, The concentration gradient fl ow battery as electricity storage system: technology potential and energy dissipation, J. Power Sources 325 (2016) 129–139.
[16] M. Tasaka, T. Hirai, R. Kiyono, Y. Aki, Solvent transport across cation-exchange membranes under a temperature difference and under an osmotic-pressure difference, J. Memb. Sci. 71 (1–2) (1992) 151–159.
[17] S. Kim, M.M. Mench, Investigation of temperature-driven water transport in polymer electrolyte fuel cell: thermo-osmosis in membranes, J. Memb. Sci. 328 (1–2) (2009) 113–120.
[18] K.D. Sandbakk, A. Bentien, S. Kjelstrup, Thermoelectric effects in ion conducting membranes and perspectives for thermoelectric energy conversion, J. Memb. Sci. 434 (2013) 10–17.
[19] J. Veerman, R.M. de Jong, M. Saakes, S.J. Metz, G.J. Harmsen, Reverse electrodialysis: comparison of six commercial membrane pairs on the thermodynamic efficiency and power density, J. Memb. Sci. 343 (1–2) (2009) 7–15.
[20] W. van Egmond, U. Starke, M. Saakes, C. Buisman, H. Hamelers, Energy efficiency of a concentration gradient flow battery at elevated temperatures, J. Power Sources 340 (2017) 71–79.
[21] A. Moura Bernardes, M.A.S. Rodrigues, J.Z. Ferreira, General Aspects of Electrodialysis, Springer, Berlin, Heidelberg, 2014, pp. 11–23.
[22] F. Leitz, M. Accomazzo, W. McRae, High temperature electrodialysis, Desalination 14 (1974) 33–41.
[23] G. Hills, P. Jacobs, N. Lakshiminarayanaiah, Non-isothermal membrane potentials, Nature 179 (1957) 96–97.
[24] T. Ikeda, Thermal membrane potential, J. Chem. Phys. 28 (1) (1958) 166.
[25] M. Tasaka, Thermal membrane potential and thermoosmosis across charged membranes, Pure Appl. Chem. 58 (12) (1986) 1637–1646.
[26] M. Tasaka, T. Mizuta, O. Sekiguchi, Mass transfer through polymer membranes due to a temperature gradient, J. Memb. Sci. 54 (1990) 191–204.
[27] K. Hanaoka, R. Kiyono, M. Tasaka, Thermal membrane potential across anion-exchange membranes in KCl and KIO_3 solutions and the transported entropy of ions, J. Memb. Sci. 82 (1993) 255–263.
[28] B.B. Sales, O.S. Burheim, S. Porada, V. Presser, C.J.N. Buisman, H.V.M. Hamelers, Extraction of energy from small thermal differences near room temperature using capacitive membrane technology, Environ. Sci. Technol. Lett. 1 (9) (2014) 356–360.
[29] M.S. Dariel, O. Kedem, Thermoosmosis in semipermeable membranes, J. Phys. Chem. 79 (4) (1975) 336–342.
[30] V.M. Barragán, S. Kjelstrup, Thermo-osmosis in membrane systems: a review, J. Non-Equilib. Thermodyn. 42 (3) (2017) 217–236.
[31] J.A. Wood, A.M. Benneker, R.G. Lammertink, Temperature effects on the electrohydrodynamic and electrokinetic behaviour of ion-selective nanochannels, J. Phys. Condens. Matter 28 (11) (2016) 114002.
[32] S. Tseng, Y.-M. Li, C.-Y. Lin, J.-P. Hsu, Salinity gradient power: influences of temperature and nanopore size, Nanoscale 8 (2016) 2350–2357.
[33] M. Tedesco, E. Brauns, A. Cipollina, G. Micale, P. Modica, G. Russo, J. Helsen, Reverse electrodialysis with saline waters and concentrated brines: a laboratory investigation towards technology scale-up, J. Memb. Sci. 492 (2015) 9–20.
[34] A. Daniilidis, D.A. Vermaas, R. Herber, K. Nijmeijer, Experimentally obtainable energy from mixing river water, seawater or brines with reverse electrodialysis, Renew. Energy 64 (2014) 123–131.
[35] M. Janssen, A. Härtel, R. Van Roij, Boosting capacitive blue-energy and desalination devices with waste heat, Phys. Rev. Lett. 113 (26) (2014) 268501.
[36] J.A.C. Weideman, S.C. Reddy, A MATLAB differentiation matrix suite, ACM Trans. Math. Softw. 26 (4) (2000) 465–519.
[37] A. Binnie, E. Poole. *The theory of the single-pass cross-flow heat interchanger*. In Mathematical Proceedings of the Cambridge Philosophical Society, 33, (Cambridge Univ Press, 1937), pp. 403–411.
[38] G.C. Benson, A.R. Gordon, A reinvestigation of the conductance of aqueous solutions of potassium chloride, sodium chloride, and potassium bromide at temperatures from 15° to 45 °C, J. Chem. Phys. 13 (11) (1945) 473–474.
[39] M.B. Sik Ali, A. Mnif, B. Hamrouni, M. Dhahbi, Electrodialytic desalination of brackish water: effect of process parameters and water characteristics, Ionics 16 (7) (2010) 621–629.
[40] M. Sadrzadeh, T. Mohammadi, Treatment of sea water using electrodialysis: current efficiency evaluation, Desalination 249 (1) (2009) 279–285.
[41] V.V. Nikonenko, A.V. Kovalenko, M.K. Urtenov, N.D. Pismenskaya, J. Han, P. Sistat, G. Pourcelly, Desalination at overlimiting currents: state-of-the-art and perspectives, Desalination 342 (2014) 85–106.
[42] L.E. Bell, Cooling, heating, generating power, and recovering waste heat with thermoelectric systems, Science 321 (5895) (2008) 1457–1461.
[43] S. Brückner, S. Liu, L. Miró, M. Radspieler, L.F. Cabeza, E. Lävemann, Industrial waste heat recovery technologies: an economic analysis of heat transformation technologies, Appl. Energy 151 (2015) 157–167.
[44] L.F. Silvester, K.S. Pitzer, Thermodynamics of electrolytes. x. enthalpy and the effect of temperature on the activity coefficients, J. Solut. Chem. 7 (5) (1978) 327–337.
[45] M. Hayashi, Temperature-electrical conductivity relation of water for environmental monitoring and geophysical data inversion, Environ. Monit. Assess. 96 (1–3) (2004) 119–128.
[46] P. Długołęcki, P. Ogonowski, S.J. Metz, M. Saakes, K. Nijmeijer, M. Wessling, On the resistances of membrane, diffusion boundary layer and double layer in ion exchange membrane transport, J. Memb. Sci. 349 (1–2) (2010) 369–379.
[47] A. Cipollina, G. Micale, Sustainable Energy from Salinity Gradients, Woodhead Publishing, 2016.
[48] R. Weast, D. Lide, M. Astle, W. Beyer, Handbook of Chemistry and Physics, 76 edition, CRC press, 1989.